Development of an aerogel-based thermal coating for the energy retrofit and the prevention of condensation risk in existing buildings

(Article begins on next page)

20 March 2024

Development of an aerogel-based thermal coating for the energy retrofit and the prevention of condensation risk in existing buildings

Stefano Fantucci, Elisa Fenoglio, Giulia Grosso, Valentina Serra, Marco Perino, Valentina Marino & Marco Dutto

Development of an aerogel-based thermal coating for the energy retrofit and the prevention of condensation risk in existing buildings

STEFANO FANTUCCI[1,*], ELISA FENOGLIO[1], GIULIA GROSSO[2], VALENTINA SERRA[1], MARCO PERINO[1], VALENTINA MARINO[3] AND MARCO DUTTO[3]

[1]*Department of Energy, Politecnico di Torino, Corso Duca degli Abruzzi 24, Torino 10129, Italy*
[2]*Politecnico di Torino, Torino, Italy*
[3]*Vimark Srl, Peveragno, Italy*

The energy retrofit of existing buildings, particularly historic and/or listed buildings, presents several issues; that is, the compatibility between the identified solutions and the heritage value or the internal space reduction (if internal interventions have to be adopted).
For this reason, an emerging method to address the target of the energy retrofit of historic buildings is the use of advanced materials characterized by high thermal insulation performance.
In the framework of a European research project (Horizon 2020), a novel aerogel-based insulating coating, particularly suitable for the mitigation of thermal bridges and for the prevention of the condensation risk, is under development.
In this article, both the laboratory and in-field research activities are described. The first was aimed at optimizing the thermohygrometric properties of the coating; the latter dealt with the results of a monitoring activity carried out on a full-scale application.
Results highlight that the internal application of 12 mm of the developed material can lead to a significant increase in indoor surface temperature (about 1.4 °C) with a decrease in the wall U-value of about 27%. Moreover, a mitigation of the thermal bridges was observed with an increase in the minimum surface temperature up to 1.6 °C.

Introduction

The building sector is responsible for nearly 40% of the total energy consumption in Europe (Directive 2010/31/EU).

About 50% of the European stock was built before the first thermal regulations in the 1970s (European Commission 2018). Italy is no exception; in fact, more than 60% of residential buildings were built before 1976, the year of the first law on energy savings, and 30% of buildings (12.5 million) are dated before 1945 (Istituto Nazionale di Statistica 2011). Therefore, a large part of the building stock is characterized by traditional non-insulated construction systems. Moreover, about 1.8% of these buildings are classified as cultural heritage, according to the definition of the Italian Legislative Decree no. 42 of 22/01/2004 pertaining to the Cultural Heritage and Landscape Code.

In the last decade, the importance of energy efficiency and thermal comfort in historical buildings has widely increased, as testified by a number of recent research studies.

Whereas energy retrofit was previously seen as a potential threat to the character and fabric of historic and traditional buildings, it is now seen largely as an opportunity to protect these buildings and respond to global environmental concerns (Webb 2017).
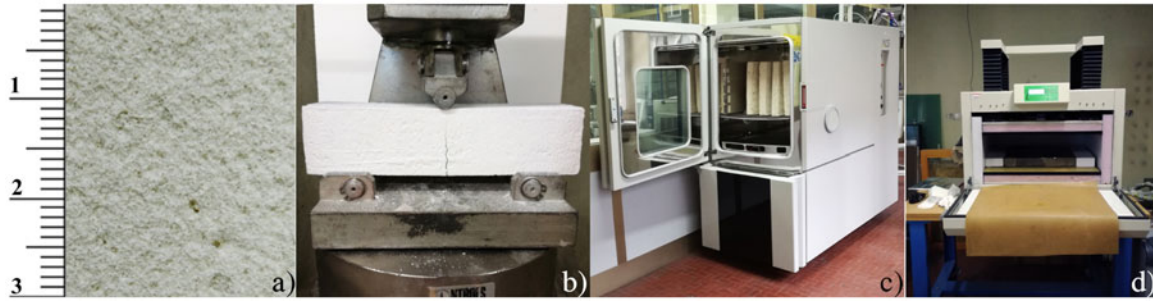
Fig. 1. a. Coating sample—surface aspect. b. Flexural strength measurement. c. Climatic chamber (ACS DM 340). d. Heat flux meter (Lasercomp FOX 600).

There is growing research activity on the challenge of matching energy efficiency measures and internal thermal comfort with the requirement of maintaining the cultural and historic significance of buildings (De Bouw et al. 2016). Among the various technical solutions to reduce thermal losses, technologies for indoor insulation are particularly suitable (Walker and Pavía 2018). Innovative materials and products, like vacuum insulation panels and aerogel-based materials, will be explored because of their high insulation potential that allows guaranteeing significant indoor space savings compared to traditional insulating materials (Fantucci et al. 2019).

In the framework of the ongoing European H2020 research project Wall-ACE, a novel aerogel-based thermal coating (to be applied together with an additional abrasive resistant top layer) has been developed, with the main aim of mitigating thermal bridges in existing buildings.

In this article, results related to thermal characterization in the lab and performance in the field are presented. The study aimed to

- optimize the thermal coating and
- demonstrate (through a full-scale application) the effectiveness of the technology to prevent the risk of surface condensation and the improvement of the whole wall thermal performance.

State-of-the-art on aerogel-based wall plasters

The use of aerogel granules as lightweight aggregates in a plaster mixture allows the final density and thermal conductivity to be drastically reduced, reaching values of $150–200\,kg/m^3$ and $0.025–0.027$ W/mK, respectively (Stahl et al. 2012; Ibrahim et al. 2015; Berardi and Nosrati 2018). Further, Buratti et al. (2014) demonstrated that by increasing the aerogel content up to 96%–99% (by volume) a density of about $115–125\,kg/m^3$ with a thermal conductivity of $0.014–0.016$ W/mK can be obtained. However, in the same study, a more mechanically performant formulation with a lower aerogel content (80%) and a thermal conductivity of 0.05 W/mK was used for in situ application.

The effective thermal insulation capability together with the plaster features (i.e., easy application on irregular substrates, relatively high compressive strength) make aerogel-based plaster a suitable candidate for the energy retrofit of historic constructions, in which the old and damaged plaster can be easily replaced with up to 4- to 6-cm aerogel plaster layers, if the existing layer has no heritage value (Ghazi Wakili et al. 2015; Schuss et al. 2017; Stahl et al. 2017; Lisitano et al. 2018).

For these reasons, in recent years, several aerogel-based plasters were developed and are currently available at least in the European Union market: FIXIT 222 (Röfix 2018a), FIXIT 244 (Röfix 2018b), Heck-Aero iP (2017), and Interbran Premium 028 (2019). They typically have a declared thermal conductivity in the range 0.028–0.048 W/mK.

Despite the fact that several studies demonstrated the high compatibility with historic buildings and the high energy retrofit capability, this technology is not, so far, largely diffused due to its high cost, which remains one of the major market limitations. In fact, it was demonstrated that for a thermal insulating plaster improved with 80% of aerogel in the mixture, the cost reached a value between €80 and €90/m² for 1 cm of thickness (Buratti et al. 2016; Ibrahim et al. 2015). However, more recent market research highlights that for larger amount of aerogel plaster/render the cost updated in 2019 is in the range €30/m²·cm (material cost only) to €60/m² per 1-cm-thick layer if the cost of application is considered (Aerogel Applications 2016; FIXIT Preisliste 2019).

A possible solution to reduce the final cost is based on minimizing the aerogel content by partially replacing it with other lightweight aggregates (de Fátima Júlio et al. 2016; Fantucci et al. 2018). Nevertheless, in most of the studies done so far, the final thermal conductivity of such products was revealed to be quite comparable with that of traditional thermal insulating plasters that are available on the market. Therefore, this solution is not optimal, and no significant benefits can be achieved compared to the state-of-the-art.

Other possible solutions aimed at reducing the final cost are based on minimization of the thickness. In a previous study by the authors (Fantucci et al. 2018), the development of an aerogel coating with a thickness between 3 and 12 mm was proposed for mitigation of thermal bridges and for slight improvement in the wall performance in terms of surface temperature of the noninsulated wall.

Methods

Five different aerogel-based thermal coatings (R0 to R4 in this article) were developed by adopting different ratios of
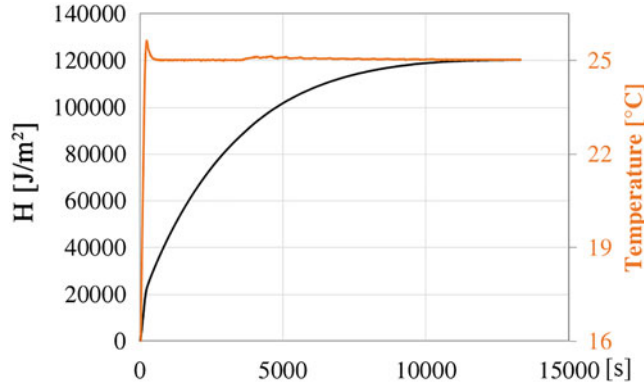
Fig. 2. Specific heat required by the sample to increase the temperature from T_1 to T_2.

mineral and organic binders. Kwark granular aerogel, produced by Enersens (2018); perlite, and glass and ceramic spheres were used, in various percentages, as lightweight aggregates (LWAs).

A first series of preliminary tests aimed at determining the thermal and mechanical properties was carried out in the laboratory. The aim was to check the compliance of the plaster with the market needs and its potentials in mitigating thermal bridges and avoiding mold growth.

Moreover, in order to test the plaster behavior under actual operating conditions, a monitoring campaign was set up and carried out on an actual building (full-scale case study) provided by Agenzia Territoriale per la Casa del Piemonte Centrale (regional agency for the Central Piedmont House).

Laboratory characterization

The laboratory measurements were aimed at determining the dry bulk density, mechanical resistance, and thermal conductivity of the developed aerogel-based plaster (Figure 1a).

The dry bulk density was measured by weighing a specimen with a known volume ($0.4 \times 0.4 \times 0.05$ m), previously dried in a climatic chamber (ACS DM 340; Figure 1c) until no weight variation of more than 0.2% occurred in a 24-h period.

Flexural and compression strength tests were carried out by Vimark S.r.l. (2019) adopting prismatic samples of $16 \times 4 \times 4$ cm according to EN 1015-11:2007 (Figure 1b).

Thermal conductivity measurement. The thermal conductivity of the dried specimens was measured according to EN 12667:2002 using a heat flux meter apparatus (Lasercomp FOX 600; Figure 1d).

Thermal conductivity measurements of the dry specimen were performed at an average temperature of 10 °C. The samples were enveloped in a polyethylene sheet in order to avoid any water vapor adsorption during the test. Moreover, the specimens were sandwiched between two natural rubber mats (2 mm thick) with a well-known thermal resistance.

This was done in order to reduce the influence of surface resistance (between the sample and the hot/cold plates) on the measured equivalent thermal conductivity of the plaster.

Specific heat capacity tests. The specific heat capacity measurements were performed according to the methodology proposed by Tleoubaev and Brzezinski (2017) using a heat flow meter. The instrument can measure the heat required to increase the temperature of the samples for a set of temperature difference. It is necessary to fix the initial temperature set-point (T_1) and the final temperature (T_2). The heat flow meter thus measures the heat absorbed by the sample to increase the temperature from T_1 to T_2 (Figure 2). The total specific heat absorbed is determined as the integration of the net specific heat flux from the two plates over time period τ; that is,

$$H = \sum_{i=1}^{N} [Q_{upper} + Q_{lower}] \tau \quad \left[\frac{J}{m^2} \right] \qquad (1)$$

Finally, the specific heat capacity c_p (J/kgK) can be determined as

$$c_p = \frac{H}{\Delta T \cdot s \cdot \rho} \quad \left[\frac{J}{kg \cdot K} \right] \qquad (2)$$

where ΔT is the difference between the first and the second set-point temperatures (°C); s is the sample thickness (m); and ρ is the sample density (kg/m³).

Specific heat capacity tests were performed on all of the aerogel-based thermal coating formulations (that is R0 to R4). ΔT was set at 10 °C, with a temperature variation of the plates from 15 °C (T_1) to 25 °C (T_2). The standard deviation of the specific heat capacity measurement was also calculated and reported within the results.

Case study building

The in-field application was aimed at investigating practical aspects related to the innovative plaster; for example, installation techniques, technical feasibility and appearance, and energy efficiency. Therefore, a monitoring campaign on a 1920s building (Figure 3) located in Turin, Italy (45°N, 7.65°E), was undertaken. From the point of view of the thermal properties, the aim of the in situ measurements was to evaluate the capacity of the optimized coating (R4) to reduce, on one hand, heat losses through the wall and, on the other hand, to mitigate thermal bridging effects and increase the wall indoor surface temperatures (during the winter time). An east-oriented room was chosen for the tests. Two identical walls, called CW (coated wall) and RW (reference wall), were analyzed. One of the two was used as a reference (RW; Figure 4a) and was left unchanged (as-built). The other (CW wall; Figure 4b) was coated with the aerogel coating (R4 formulation).

The coating was prepared and applied on the CW and the adjacent thermal bridge (vertical intersection between the wall and window). In order to improve the adhesion of the thermal coating on the existent wall, a mono-component primer in thin layer was firstly applied (Figure 5a). The
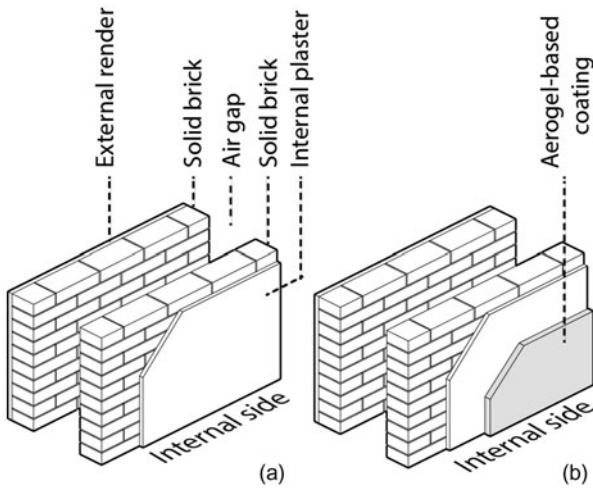
Fig. 3. The 1920s test building in Torino.

Fig. 4. a. Reference wall (RW). b. Coated wall (CW).

Fig. 5. a. Primer application. b. Mixing. c. Coating application. d. Final thickness.

thermal coating, mechanically mixed in a ∼1:1 water ratio, was manually applied to reach a thickness of ∼12 mm (Figures 5b–5d). The measurements were directly performed on the aerogel-based coating layer without applying an abrasive-resistant top layer.

In-field monitoring

The monitoring campaign was carried out for about 2 months in the winter period. Temperature and specific heat flux sensors were placed both on the CW and RW and on the thermal bridges. To avoid placing the sensors in a non-homogeneous area of the wall, a preliminary set of thermographic tests was performed analogous to thermal insulating plasters analyses carried out by Ghazi Wakili et al. (2014) and Fenoglio et al. (2018). As shown in Figure 6, two heat flux sensors (HFP01) were located in the center of the walls. T-type thermocouples were used to measure air and surface temperatures, both on the walls and in the thermal bridges zones.

Thermocouples were also placed at the interface between the thermal coating and the pre-existing wall (CW; Figure 6).

A pyranometer sensor was used to measure the incident solar radiation. The indoor temperature was kept at 23 °C ± 1 °C for the whole monitoring period, in order to achieve a temperature difference between the indoors and the outdoors that was high enough to measure the specific heat fluxes with sufficient accuracy. To avoid the influence of solar radiation on the monitored surfaces, the window shutters were kept closed during the measuremnts.

The continuous average method (ISO 9869-1:2014) was used to assess the thermal transmittance U (Equation 3) and thermal conductance C (Equation 4) at the center of the wall:

$$U = \frac{\sum_{J=1}^{n} q_J}{\sum_{J=1}^{n} (T_{aij} - T_{aej})} \qquad (3)$$

$$C = \frac{\sum_{J=1}^{n} q_J}{\sum_{J=1}^{n} (T_{sij} - T_{sej})} \qquad (4)$$

where q_J is the measured specific heat flux; T_{sij} and T_{sej} are the internal and external surface temperatures, respectively;

and T_{aij} and T_{aej} are the internal and external air temperatures, respectively.

Results and discussion

Laboratory results

Laboratory tests showed that the aerogel coatings are characterized, in general, by good thermophysical properties (Table 1). The density of the dry specimens was ~50% lower than that of traditional thermal insulating coating without aerogel (R0; Table 1).

As it is possible to observe from Table 1, the optimized formulation with the Kwark aerogel (R4) has an equivalent thermal conductivity of 0.051 W/mK. This corresponds to a reduction of the equivalent thermal conductivity of about 62% compared to the reference R0 formulation.

With regard to mechanical properties, the flexural strength of R4 is equal to 0.8 MPa, with a negligible reduction in performance with respect to the R0 formulation.

The intermediate optimization steps that were implemented for switching from the reference formulation, R0, to the optimized one, R4, were represented by the following:

- Replacement of part of the LWA with the aerogel (from R0 to R1). This provided a slight improvement in the thermal performance (~13%) with a reduction in the dry bulk density from 617 to 577 kg/m^3.
- Replacement of part of the mineral binders with organic binders. This led to a reduction in the thermal conductivity of about a 44% (from R2 to R3) and allowed a significant reduction in density. Moreover, the differences in binders also resulted in an increase in the specific heat capacity of about 30%.

In-field monitoring results

The temperature at the center of the wall and the specific heat fluxes were analyzed considering the entire monitoring period from December 21 to March 3 (Figure 7). Moreover, additional analyses were carried out focusing on the potential thermal bridge mitigation attainable with the thermal coating finish.

Center of wall thermal performance. A box plot analysis of the wall temperatures at the center of the wall and the specific heat fluxes of the CW and RW are shown in Figure 8.

The monitored data highlight that the application of the thermal coating finish allows

- an increase of about 1.4 °C and 0.9 °C in the median and minimum indoor surface temperatures, respectively (improvement in indoor thermal comfort and reduction in surface condensation and mold risk; Figure 8a).
- a decrease of about 1 °C and 1.4 °C in the median and minimum outdoor surface temperatures, respectively (this aspect mainly concerns the durability of the outer plaster layer that might be exposed to freeze–thaw cycles in a cold climate; Figure 8b).
- a reduction of about 30% in the median value of the center of wall heat losses during the winter, which can provide a reduction in heating energy demand (Figure 8c).

Figure 9 shows the time evolution of the *U*-values and of the conductance of the walls determined at each time step using Equations 3 and 4. The measured *U*-values of the CW and RW were 0.90 and 1.22 W/(m^{2}K), respectively. From a practical point of view, the addition of about 12 mm of aerogel coating finish resulted in reductions of ~37% and ~27% in the wall thermal conductance and thermal transmittance, respectively. Particular care has to be taken in relation to the maturation time of the layer. As observed during the field tests, about 2 months is needed for the water in the mixture to be removed. During this time, the moisture content is higher than that in normal operating conditions, which negatively affects the thermal performance of the layer. All data presented in this article are from measurements performed after 2 months, near the final condition of the wall.
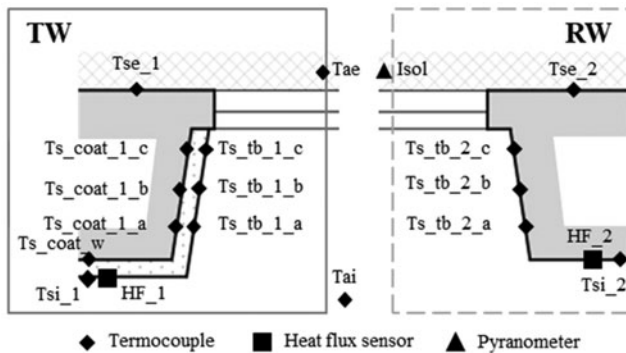

Fig. 6. Sensor types and positions.

Table 1. Results of laboratory measurements.

Sample name	Binders	LWA (type)	ρ (kg/m^3)	$\lambda_{10°C}$ (W/mK)	c_p (J/kgK)[a]	Flexural strength (MPa)
R0	Mineral	Mineral	617	0.138	1000	0.8
R1	Mineral	Mineral + Aerogel	577	0.120	740	1
R2	Mineral	Mineral + Aerogel	495	0.102	810	—
R3	Mineral + Organic	Mineral + Aerogel	369	0.057	1050	1
R4	Mineral + Organic	Mineral + Aerogel	326	0.051	1070	0.8

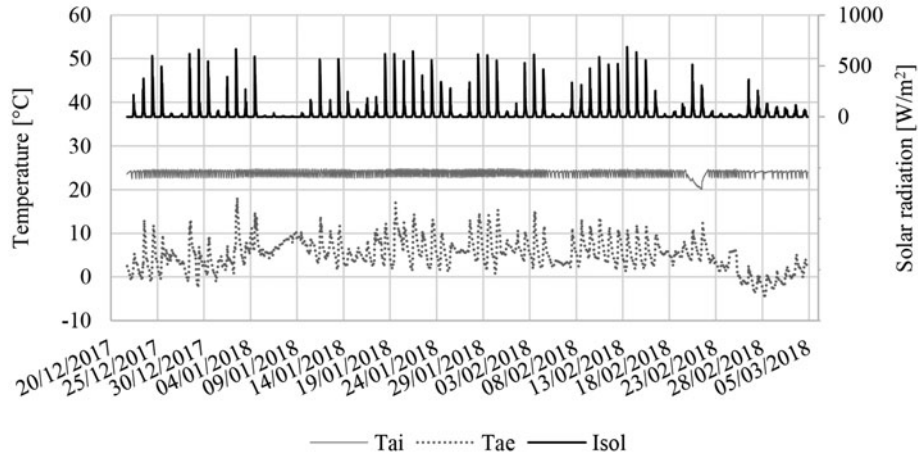Note: [a]The relative standard deviation for the c_p measurement was ~0.2%.
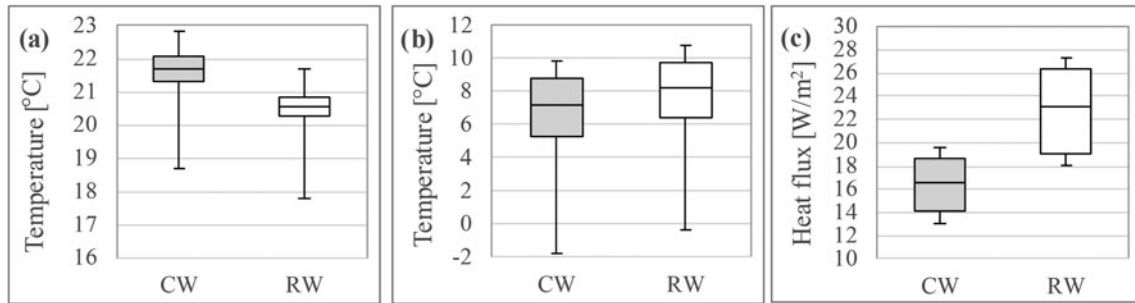
Fig. 7. Boundary conditions.

Fig. 8. a. Box plot analysis of the monitored indoor surface temperature. b. Box plot analysis of the monitored external surface temperature. c. Box plot analysis of the monitored indoor surface specific heat fluxes.
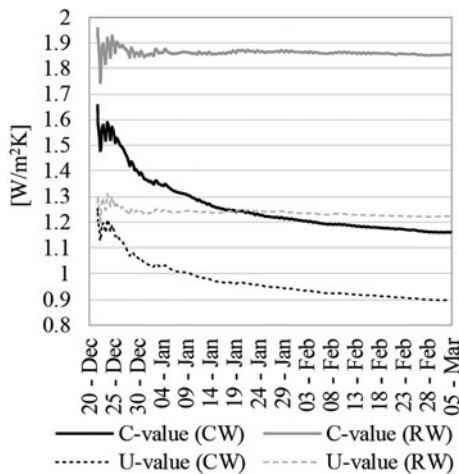

Fig. 9. Measured thermal conductance *C* and thermal transmittance *U* of the RW and CW.

Mitigation of thermal bridges. The intersection between the wall and the window frame has been identified as the area mostly affected by the presence of the thermal bridge. For this reason, the surface temperatures of the wall side were analyzed in detail (Figure 10a). Firstly, the infrared images of the CW and RW thermal bridges were compared.

Results are shown in Figures 10b and 10c; the temperature increased significantly due to the presence of the R4 thermal coating.

Figure 11 shows the box plot analysis of the surface temperatures of the CW and RW configurations.

The monitored results confirm that the application of the aerogel-based thermal coating allows the temperature in the proximity of the thermal bridge to be notably increased. In particular, an effective increase in the minimum surface temperature 5 cm from the construction node (sensor Ts_tb_c), from 15.3 °C to 16.9 °C, can be observed, whereas the difference is negligible at 15 cm (sensor Ts_tb_b). Conversely, at 25 cm from the construction node (sensor Ts_tb_a), the application of the thermal coating finish resulted in a slightly lower surface temperature.

An additional analysis was performed to determine the potential mitigation of the surface condensation risk. This study was performed for a point 5 cm from the node, and the results are shown in Figure 12. The cumulative frequency distribution of the difference between the monitored surface temperature and the dew point temperature for different indoor relative humidity classes (from 60% to 70%) are plotted. The analysis highlighted that
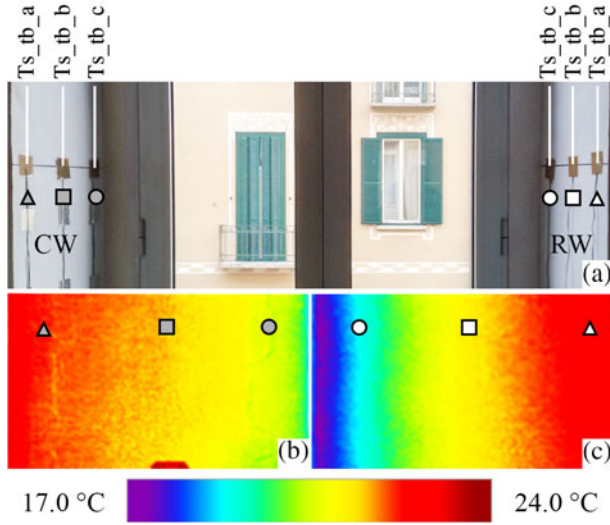
Fig. 10. a. Thermocouples installed in the area of thermal bridges. b. Infrared image of CW thermal bridge. c. Infrared image of RW thermal bridge.
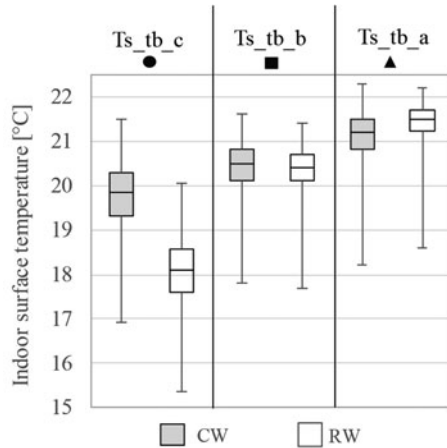

Fig. 11. Box plot analysis of the surface temperatures of the thermal bridge.

- no surface condensation occurred at 60% of indoor relative humidity for both wall configurations (RW and CW).
- condensation occurred for about 30% of the time in the RW at 70% indoor relative humidity, whereas the surface condensation risk was neutralized in the CW.

Conclusions

In the framework of the Horizon 2020 project 'Wall ACE', a novel aerogel-based thermal coating was developed. As a first research step, the main physical properties of a set of four mixtures were assessed through laboratory analyses. The results allowed optimization of the material properties
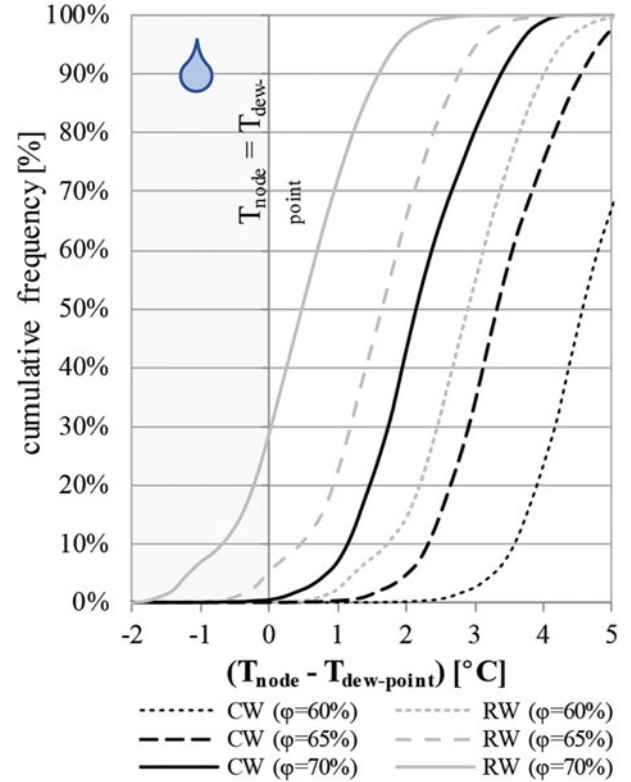

Fig. 12. Cumulative frequency distributions of the difference between the node temperature (Ts_tb_c) and the dew point temperature for different indoor relative humidity conditions.

and selection of a mixture that presents a thermal conductivity of about 0.05 W/mK. Furthermore, the best performing material was applied for an external wall energy retrofit in a 1920s demonstration building in Turin, Italy. The thermal behavior of the retrofitted wall was monitored during the winter season, and its performance was compared with that of an uncoated reference wall. The obtained results highlight that the application of a thin thermal coating finishing layer can lead to a significant increase in the median indoor surface temperature (about 1.4 °C), with a decrease in the wall thermal transmittance of about 27%. Moreover, mitigation of the effect of the thermal bridge was also observed with an increment in the minimum node surface temperature (wall–window frame) of up to 1.6 °C. The obtained results highlighted that the developed thermal coating can provide a non-negligible reduction in heat losses through the wall.

Moreover, the aerogel-based coating represents a promising solution to mitigate the adverse effects of thermal bridges on the condensation risk, even when the indoor environment is characterized by high relative humidity. These results are a good argument for the suitability of the developed product for the application in all buildings in which usual thick internal insulating solutions cannot be addressed due to space, historical, and technical constraints.

Acknowledgments

Funding

References

Aerogel Applications. 2018. http://aerogelanwendungen.ch/en/application/.

ASTM C1784-14. *Standard Test Method for Using a Heat Flow Meter Apparatus for Measuring Thermal Storage Properties of Phase Change Materials and Products*.

Berardi, U., and R.H. Nosrati. 2018. Long-term thermal conductivity of aerogel of aerogel-enhanced insulating materials under different laboratory aging conditions. *Energy* 147:1188–1202.

Buratti, C., E. Moretti, and E. Belloni. 2016. *Nano and Biotech Based Materials for Energy Building Efficiency*. Aerogel plasters for building energy efficiency. F. Pacheco Torgal, C. Buratti, S. Kalaiselvam, C.-G. Granqvist, and V. Ivanov, eds. Cham, Switzerland: Springer International Publishing. Chapter 2. https://doi.org/10.1007/978-3-319-27505-5_2.

Buratti, C., E. Moretti, E. Belloni, and F. Agosti. 2014. Development of innovative aerogel based plasters: Preliminary thermal and acoustic performance evaluation. *Sustainability* 6:5839–52. doi:10.3390/su6095839.

De Bouw, M., S. Dubois, L. Dekeyser, and Y. Vanhellemont. (eds.). 2016. *Proceedings of Energy Efficiency and Comfort of Historic Buildings (EECHB 2016)*, Brussels, Belgium, October 19–21, 2016.

2004 Italian Legislative Decree 22 gennaio 2004, n. 42. Codice dei beni culturali e del paesaggio, ai sensi dell'articolo 10 della legge 6 luglio 2002, n. 137. *Gazzetta Ufficiale* 45(Suppl.).

de Fátima Júlio, M., A. Soares, L.M. Ilharco, I. Flores-Colen, and J. de Brito. 2016. Aerogel-based renders with lightweight aggregates: Correlation between molecular/pore structure and performance. *Construction and Building Materials* 124(15):485–495.

The European Parliament. 2010. Directive 2010/31/EU of the European Parliament and the Council of 19 May 2010 on the energy performance of buildings. http://eur-lex.europa.eu/legalcontent/EN/TXT/PDF/?uri=CELEX:32010L0031&from=EN.

Enersens. 2018. Aerogel particles Kwark. http://enersens.fr/en/home/silica-aerogel-particles/.

European Commission. 2018. EU buildings factsheets: Building stock characteristics. https://ec.europa.eu/energy/en/eu-buildings-factsheets.

Fantucci, S., E. Fenoglio, F. Isaia, V. Serra, M. Perino, M. Dutto, and V. Marino. 2018. *Development of aerogel based internal thermal plasters for the energy retrofit of existing buildings: First results*. COBEE, Melbourne, Australia, February 5–9.

Fantucci, S., S. Garbaccio, A. Lorenzati, and M. Perino. 2019. Thermo-economic analysis of building energy retrofits using VIP—Vacuum insulation panels. *Energy and Buildings* 196:269–79. https://doi.org/10.1016/j.enbuild.2019.05.019.

Fenoglio, E., S. Fantucci, V. Serra, C. Carbonaro, and R. Pollo. 2018. Hygrothermal and environmental performance of a perlite-based insulating plaster for the energy retrofit of buildings. *Energy and Buildings* 179(15):26–38. https://doi.org/10.1016/j.enbuild.2018.08.017.

FIXIT Preisliste. 2019. Preisliste. https://www.fixit.ch/Home/Services/Downloads/Preisliste.

Ghazi Wakili, K., B. Binder, M. Zimmermann, and C. Tanner. 2014. Efficiency verification of a combination of high performance and conventional insulation layers in retrofitting a 130-year old building. *Energy and Building* 82:237–42. http://dx.doi.org/10.1016/j.enbuild.2014.06.050.

Ghazi Wakili, K., Th. Stahl, E. Heiduk, M. Schuss, R. Vonbank, U. Pont, C. Sustr, D. Wolosiuk, and A. Mahdavi. 2015. High performance aerogel containing plaster for historic buildings with structured façades. *Energy Procedia* 78:949–954.

Heck. 2017. Heck-Aero iP. http://baunativ.de/pdf_de/AERO_iP_TM.pdf.

Ibrahim, M., P. Henry Biwole, P. Achard, E. Wurtz, and G. Ansart. 2015. Building envelope with a new aerogel-based insulating rendering: Experimental and numerical study, cost analysis, and thickness optimization. *Applied Energy* 159:490–501.

Interbran Premium 028. 2019. https://www.agitec.ch/page/PDF-Dateien/Technische-Merkblaetter/Deutsch/TDB_Interbran_Premium_Daemmputz_028.pdf?m=1527205755&

Istituto Nazionale di Statistica. 2011. National census. http://dati-censimentopopolazione.istat.it/Index.aspx.

Lisitano, I.M., D. Laggiard, S. Fantucci, V. Serra, C. Bartolozzi, E.M. Lorenzo, and M. Sabín Díaz. 2018. *Energy in cultural heritage: The case study of Monasterio de Santa Maria de Monfero in Galicia. REHABEND 2018*, Cáceres, Spain May 15–18, 2018.

Röfix. 2018a. FIXIT 222. https://www.roefix.it/var/fixitgruppe/storage/ilcatalogue/files/pdf/ITIT/Scheda_tecnica_FIXIT_222_Aerogel_Intonaco_altamente_isolante_Intonaco__DC0030070.PDF.

Röfix. 2018b. FIXIT 244. https://www.roefix.at/var/fixitgruppe/storage/ilcatalogue/files/pdf/ATDE/Technisches_Merkblatt__TM__FIXIT_244__Aerogel_D%C3%A4mmputz_DC0056784.PDF.

Schuss, M., U. Pont, and A. Mahdavi. 2017. Long-term experimental performance evaluation of aerogel insulation plaster. *Energy Procedia* 132:508–13. https://doi.org/10.1016/j.egypro.2017.09.696.

Stahl, Th., S. Brunner, M. Zimmermann, and K. Ghazi Wakili. 2012. Thermo-hygric properties of a newly developed aerogel based insulation rendering for both exterior and interior applications. *Energy and Buildings* 44:114–117.

Stahl, T., K. Ghazi Wakili, S. Hartmeier, E. Franov, W. Niederberger, and M. Zimmermann. 2017. Temperature and moisture evolution beneath an aerogel based rendering applied to a historic building. *Journal of Building Engineering* 12:140–146. http://dx.doi.org/10.1016/j.jobe.2017.05.016.

Tleoubaev, A., and A. Brzezinski. 2007. Thermal diffusivity and volumetric specific heat measurements using heat flow meter instruments for thermal conductivity. *Proceedings of 29th International Thermal Conductivity Conference*, Birmingham, AL, June 24–27.

ISO 9869-1:2015. *Thermal Insulation—Building Elements—In-Situ Measurement of Thermal Resistance and Thermal Transmittance. Part 1: Heat Flow Meter Method*. Geneva, Switzerland: ISO.

EN 1015-11:2007. *Methods of Test for Mortar for Masonry— Determination of Flexural and Compressive Strength of Hardened Mortar*. Geneva, Switzerland: ISO.

EN 12667:2002 *Thermal Performance of Building Materials and Products. Determination of Thermal Resistance by Means of*

Guarded Hot Plate and Heat Flow Meter Methods. Products of High and Medium Thermal Resistance. Brussels: CEN - European Committee for Standardization.

Vimark. 2019. Produttori di materiali, sistemi e servizi nel settore edile [Producer of materials, system and services for the building sector]. https://www.vimark.com/it/.

Walker, R., and S. Pavía. 2018. Thermal and moisture monitoring of an internally insulated historic brick wall. *Building and the Environment* 133:178–86.

Webb, A.L. 2017. Energy retrofits in historic and traditional buildings: A review of problems and methods, *Renewable and Sustainable Energy Reviews* 77:748–59.